J. Membrane Biol. 37, 361–396 (1977)

The Kinetic Mechanism of Action of an Uncoupler of Oxidative Phosphorylation

Fredric S. Cohen*, Moisés Eisenberg, and Stuart McLaughlin

Health Sciences Center, S.U.N.Y., Stony Brook, New York 11794

Received 7 March 1977; revised 20 May 1977

Summary. The chemiosmotic hypothesis predicts that the mechanism by which weak acids uncouple oxidative phosphorylation in mitochondria is identical to the mechanism by which they transport hydrogen ions across artificial bilayer membranes. We report here the results of a kinetic study of uncoupler-mediated hydrogen ion transport across bilayer membranes. We made electrical relaxation measurements on black lipid membranes exposed to the substituted benzimidazole 5,6-dichloro-2-trifluoromethylbenzimidazole. The simplest model consistent with our experimental data allowed us to deduce values for adsorption coefficients and rate constants. Our major conclusions are that the back diffusion of the neutral species is the rate limiting step for the steady state transport of hydrogen ions, that both the neutral and charged forms of the uncoupler adsorb strongly to the interfaces, and that the reactions at the membrane-solution interfaces occur sufficiently rapidly for equilibrium to be maintained. Independent measurements of the adsorption coefficients of both the neutral and anionic forms of the weak acid and also of the permeability of the membrane to the neutral form agreed well with the values deduced from the kinetic study.

The chemiosmotic hypothesis (e.g., Mitchell, 1961, 1966, 1972; Greville, 1969; Skulachev, 1971; Harold, 1972; Racker, 1976) predicts that an electrochemical gradient of hydrogen ions is formed across the inner membrane of the mitochondrion as a result of substrate oxidation and that the passive movement of hydrogen ions into the organelle through an ATPase complex generates ATP from ADP. One of the attractive features of the hypothesis is that it should be easy to disprove if untrue. Three necessary conditions for the hypothesis to be valid are (i) that oxidation produce an electrochemical gradient of hydrogen ions, (ii) that the movement of protons through the ATPase be capable of producing ATP and (iii) that the inner membrane of the mitochondrion be re-

* *Present address:* Department of Physiology, A. Einstein College of Medicine, Bronx, N.Y. 10461.

latively impermeable to protons and thus not provide a shunt for the movement of these ions. Mitchell and Moyle (1967*a*) have demonstrated by direct measurement that oxidation does indeed produce an acidification of the medium bathing the mitochondria, and Liberman, Topaly, Tsofina, Jasaitis and Skulachev (1969) have used lipid soluble ions to infer that the inside of a mitochondrion is electrically negative with respect to the bathing solution. Racker and Stoeckenius (1974) have demonstrated that the mitochondrial ATPase, when incorporated into a phospholipid vesicle, can produce ATP upon exposure to an electrochemical gradient of protons. Finally, the experiments of Mitchell and Moyle (1967*b*) demonstrate that the inner mitochondrial membrane is relatively impermeable to protons.

The success of the chemiosmotic hypothesis in withstanding these three critical tests suggests that a quantitative examination of other predictions would be worthwhile. The lipids in a mitochondrion have been shown to be arranged in the form of a bilayer (Blazyk & Steim, 1972; Hsia *et al.*, 1972). It follows, as a corollary of the chemiosmotic hypothesis, that all compounds which transport protons across artificial bilayers should be able to dissipate the electrochemical gradient of protons across the inner mitochondrial membrane and, therefore, act as uncouplers of oxidative phosphorylation. There should, furthermore, be a correlation between the concentration of uncoupler required to enhance the conductance of a bilayer membrane and the concentration required to uncouple a mitrochondrion. Skulachev (1971) did observe such a correlation, whereas Ting, Wilson and Chance (1970), who studied several of the same uncouplers, did not. We will present elsewhere experimental evidence (McLaughlin, S., Cohen, F., Dilger, J., & Eisenberg, M., *manuscript in preparation*) which supports the observations of Skulachev (1971). An excellent correlation has also been observed (Cunarro & Weiner, 1975) between the concentration of weak acid required to induce proton transport across a mitrochondrial membrane (as measured by the swelling of poisoned mitochondria) and the concentration required to stimulate respiration.

In spite of this correlation, not all investigators are convinced about the mechanism of action of these uncouplers on biological systems (e.g., Kraayenhof & Arents, 1977; Kessler *et al.*, 1977). Some investigators favor the idea that these molecules act by virtue of their ability to bind to specific sites (e.g., Wilson & Brooks, 1970). Perhaps the strongest evidence in favor of this point of view has been obtained by Hanstein & Hatefi (1974*a*, *b*) and Hanstein (1976). They synthesized a radioactive,

photoaffinity labelled analog of 2,4-dinitrophenol, namely 2-azido-4-nitrophenol (NPA) and showed that NPA binds to specific proteins located in the inner membrane of the mitochondria. They concluded from these experiments that uncouplers could produce their effects on mitochondria by binding to specific proteins rather than by reducing the electrochemical gradient of protons across the inner membrane. The continuing debate about the mechanism of action of uncouplers on biological systems implies that quantitative measurements of the pH and concentration dependence of the efficacy of a series of closely related uncoupler homologs on both the artificial and biological membranes would be valuable, perhaps necessary, to help resolve the issue. The substituted benzimidazoles were selected for a number of reasons: they are extremely potent uncouplers, analogs exist with widely different pK values, they do not change the surface charge density or surface potential of membranes, and relaxations in the current can be observed in voltage clamp experiments on black lipid membranes. This latter property allows one to deduce the kinetic parameters of these uncouplers on bilayer membranes. Such kinetic measurements use the approach originally developed by Eigen and his colleagues, an approach which was first applied to carrier-mediated transport across bilayer membranes by Stark, Ketterer, Benz and Läuger (1971). (Relaxations were first observed with an uncoupler by Bamberg (1973)). We studied the substituted benzimidazole 5,6-dichloro-2-trifluoromethylbenzimidazole (DTFB) in some detail. We begin by considering the equilibrium properties of this uncoupler (Büchel, Korte & Beechey, 1965).

Materials and Methods

Bacterial phosphatidyl ethanolamine, dioleoyl phosphatidyl choline and bovine cardiolipin were obtained from Supelco (Belefonte, Pa.). Egg phosphatidyl choline was prepared by the method of Singleton, Gray, Brown and White (1965) and 5,6-dichloro-2-trifluoromethylbenzimidazole (DTFB) was synthesized using a modification of the procedure of Acheson, Taylor and Tomlinson (1958).

The aqueous solutions were prepared with 18 Mohm cm "Super Q" (Millipore Corporation) water and contained, unless otherwise specified, 1 M NaCl buffered with 0.1 M phosphate, citrate and Tris.

The planar membranes were formed at room temperature (22–23 °C) in a teflon chamber from a 25 mg/ml solution of PE in *n*-decane (Supelco). A disposable pipette was used to deposit the lipid on the orifice and to form the membrane. The pipette was flamed immediately prior to use to remove organic impurities. The area of the membrane (1–2 mm^2) was measured with an eyepiece reticule attached to a Wild M 5 stereomicroscope. The contents of the chamber were stirred with Teflon coated magnets. The uncoupler was added to the aqueous solutions in the form of a concentrated ethanolic

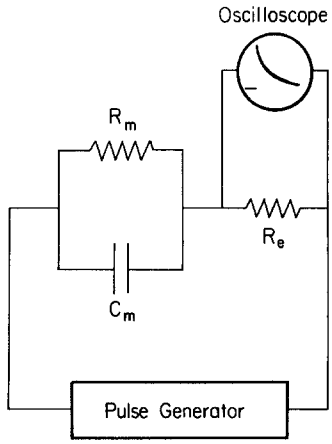

Fig. 1. Schematic diagram of the circuit used to observe current relaxations. *See text* for details

solution. The final concentration of ethanol never exceeded 0.5%, and control experiments indicated that this concentration did not measurably affect the membrane resistance.

The relaxation experiments were performed by the method described by Stark *et al.*, (1971). As illustrated in Fig. 1, an external resistor, R_e, was placed in series with the planar bilayer of resistance R_m and capacitance C_m. At a time $t=0$, a single voltage pulse of known amplitude was applied across the system with a Wavetek 164 function generator. The current through the external resistor was monitored with a Tektronix 7623 A storage oscilloscope and the trace was recorded on Polaroid film for analysis. Two Ag/AgCl electrodes were used routinely. Identical results were obtained in experiments performed with a four electrode system as a control against the possibility of electrode polarization.

The response of the dummy circuit described by Ketterer, Neumcke and Läuger (1971) to a square voltage voltage pulse was solved by J. Dilger by means of Laplace transforms. The response consisted of two exponential relaxations and a steady state current. By choosing appropriate resistors and capacitors we could mimic the electrical response of a bilayer membrane to a voltage pulse; a rapid capacitive transient, followed by an exponential relaxation and a steady state current due to DTFB. By testing that the relaxations measured with this dummy circuit agreed with the theoretically predicted relaxations, we controlled against possible artifacts in the electronics (e.g., the possibility that the amplifier was overloaded by the initial transient).

The membrane potentials produced when the values of the pH in the two solutions were different were recorded via calomel electrodes with a Keithley 602 electrometer. A pH electrode in one chamber monitored the pH.

The multilamellar vesicles for the microelectrophoresis experiments were prepared by diluting a concentrated solution of egg phosphatidyl choline (in chloroform) in 2 ml of spectroscopically pure ethanol, drying the mixture in a rotary evaporator, adding the desired solution and three glass beads, then shaking the flask for a few minutes (Bangham, Hill & Miller, 1974). The electrophoretic mobilities were measured on a commercially available (Rank Bros., Bottisham, Cambridge, U.K.) cylindrical cell apparatus based on the design of Bangham, Flemans, Heard and Seaman (1958). All measurements were made at the theoretical "stationary layer" (e.g., Shaw, 1969). Experi-

ments were performed alternately on vesicles in the control (10^{-3} M NaCl, 10^{-4} M Tris and phosphate buffers) and in the experimental solutions (control solution plus DTFB). The concentrations of DTFB ranged from 2.5 to 25 μM. The zeta potential, ζ, the potential at the hydrodynamic plane of shear, was calculated from the Helmholtz-Smoluchowski equation: $\zeta = \eta u/\varepsilon_0 \varepsilon_r$, where η is the viscosity and ε_r is the dielectric constant of the aqueous phase, u is the mobility of the vesicle and ε_0 is the permittivity of free space. All variables are expressed in S.I. units in this equation. Shaw (1969), Aveyard and Haydon (1973) or Overbeek and Wiersema (1967) may be consulted for a derivation of the equation.

The single walled vesicles (e.g., Huang, 1969) used for the adsorption studies were prepared by sonicating egg phosphatidyl choline in the indicated salt solution for 45 min with an Ultrasonic Devices Model W140 sonicator. The sonication was performed under a nitrogen atmosphere in an ice bath to minimize lipid oxidation. The solution was then centrifuged at 35,000 rpm for 60 min in a Beckman L2-75B ultracentrifuge to remove metallic fragments, undispersed lipid, and larger vesicles.

The dialysis membranes were prepared by boiling the tubing (Fisher, Cat. No. 8-667B) in a 10 mM $NaHCO_3$, 10 mM ethylenediaminetetraacetic acid solution for two hr, then rinsing thoroughly with distilled water. We discovered, in control experiments, that DTFB adsorbed significantly to commercially available dialysis chambers constructed from perspex and used, therefore, dialysis chambers machined from Teflon. Control experiments demonstrated that DTFB equilibratated across the dialysis membrane within four hr and did not adsorb significantly to either the chamber or the dialysis membrane. The concentrations of DTFB were determined with a Beckman Acta III spectrophotometer at 292 nm and 258 nm for the A^- and HA species, respectively.

Equilibrium Theory

Conductance. The equilibrium model under consideration was originally formulated by Lea and Croghan (1969) and by Finkelstein (1970). We assume that the following two reactions occur in the aqueous phases:

$$HA \rightleftharpoons H^+ + A^-, \qquad K_{HA} = \frac{[H^+][A^-]}{[HA]} \tag{1}$$

$$HA_2^- \rightleftharpoons HA + A^-, \quad K_{HA_2} = \frac{[HA][A^-]}{[HA_2^-]} \tag{2}$$

where A^- represents the anion and HA the undissociated acid. The total concentration of uncoupler, $[A^{TOT}]$, is given by:

$$[A^{TOT}] = [A^-] + [HA] + 2[HA_2^-]. \tag{3}$$

By combining Eqs. (1)–(3) we obtain:

$$\frac{[HA_2^-]}{\left(1 - \frac{2[HA_2^-]}{[A^{TOT}]}\right)^2} = \frac{K_{HA}[H^+][A^{TOT}]^2}{K_{HA_2}(K_{HA} + [H^+])^2}. \tag{4}$$

If we assume that $[HA_2^-] \ll [A^{TOT}]$, an assumption we justify *a posteriori,* it follows that:

$$[HA_2^-] = \frac{K_{HA}[H^+][A^{TOT}]^2}{K_{HA_2}(K_{HA}+[H^+])^2}. \tag{5}$$

We now assume that only the HA_2^- species carries current across the membrane and that the uncoupler does not significantly change the electrostatic potential within the membrane. Both of these assumptions are consistent with all the experimental results we have obtained for the uncoupler under consideration. If the conductance measured on application of a voltage V, after a time t, $G_{V,t}$, is estimated in the limit that V, $t \to 0$, it follows that:

$$G_{0,0} \propto \frac{[H^+][A^{TOT}]^2}{(K_{HA}+[H^+])^2}. \tag{6}$$

McLaughlin (1972) discusses the assumptions inherent in the equilibrium model in more detail. We merely note here that Eq. (6) will also be valid for voltages and times greater than zero if the movement of the charged permeant species across the membrane is the rate limiting step when a voltage is applied (e.g., Ciani *et al.*, 1973). This simple model (Eq. 6) predicts that the conductance should depend on the square of the total uncoupler concentration and have a maximum at a pH equal to the pK of the weak acid.

Membrane Potential. If, as assumed above, the only charged membrane permeable species is the HA_2^- complex, the potential difference, ϕ, between the two membrane solution interfaces is given by the Nernst expression:

$$\phi = \frac{RT}{F} \ln \frac{[HA_2^-]'_{if}}{[HA_2^-]''_{if}} \tag{7}$$

where R, T and F have their usual meaning, and the concentrations of the HA_2^- species at the left and right hand interfaces are denoted by $[HA_2^-]'_{if}$ and $[HA_2^-]''_{if}$, respectively. If (i) the aqueous solutions are well buffered, (ii) the pH is not too far to the alkaline side of the pK of the weak acid, (iii) the movement of the HA species is limited by diffusion through the aqueous unstirred layers (e.g., Fig. 2*c* of McLaughlin & Eisenberg, 1975), it follows, as discussed in more detail in Foster and

McLaughlin (1974; pp. 159–161), that the measurable potential difference, V, between the two bulk aqueous phases is given by:

$$V = \frac{RT}{F} \ln \frac{[H^+]''}{[H^+]'} \tag{8}$$

where $[H^+]''$ and $[H^+]'$ denote the concentrations of hydrogen ions in the right and left hand bulk aqueous phases, respectively. It also follows from assumptions (i–iii) that a difference in the concentration of uncoupler should produce zero membrane potential when the pH is the same on both sides of the membrane.

Equilibrium Results

We test here the three predictions of the "equilibrium" model discussed in the preceding section. Fig. 2 illustrates that the conductance does depend quadratically on the concentration of DTFB in the aqueous

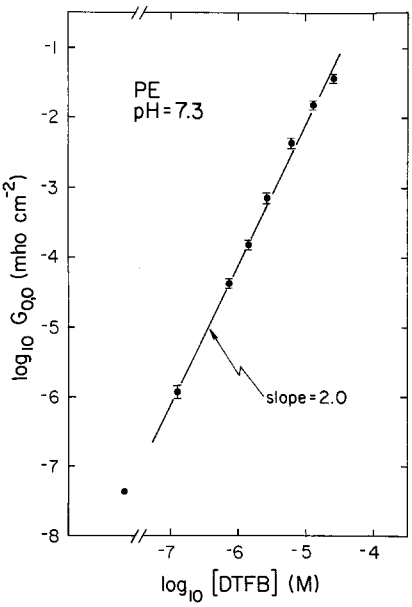

Fig. 2. The initial ohmic conductance, $G_{0,0}$, of a black lipid membrane formed from PE is a quadratic function of the aqueous concentration of the uncoupler DTFB. The last squares linear regression line through the points has a slope of 2.0, in agreement with the theoretical prediction of Eq. (6). The error bars represent the SD of a least three measurements

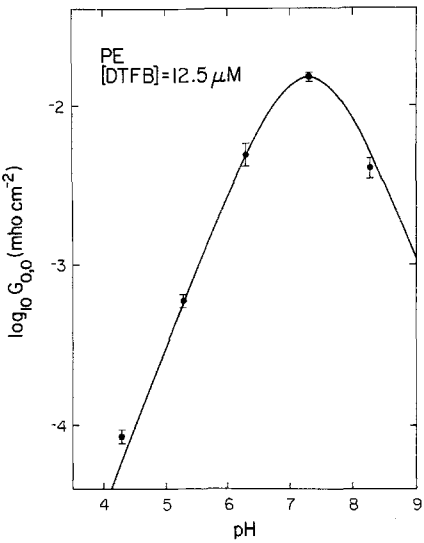

Fig. 3. Dependence of the initial ohmic conductance, $G_{0,0}$ of a black lipid membrane formed from PE on pH. The curve through the points was drawn according to Eq. (6), normalized to the conductance value at pH 7.3. The error bars represent the SD of at least three measurements

phase, as predicted by Eq. (6).[1] A quadratic dependence of conductance on concentration was observed for all pH values lower than the pK and at pH 8.3 for concentrations higher than 10^{-6} M.

Fig. 3 illustrates that for values of the pH between 4.3 and 8.3 the conductance depends on pH in the manner predicted by Eq. (6). At lower values of the pH the phosphate group on the membrane is titrated and at higher values of the pH the amine group is titrated, which changes the electrostatic surface potential (Szabo, Eisenman, McLaughlin & Krasne, 1972).

The other predictions of the model are also borne out by experiment. A difference in the concentration of H^+ produces the expected Nernst potential, provided the pH is lower than 9. A difference in the concentration of uncoupler produces no membrane potential when the pH (<9) is the same on both sides of the membrane. Both of these observations are due, as discussed elsewhere (Foster & McLaughlin, 1974) to

1 As discussed below, exponential relaxations in the current were noted for the three highest concentrations graphed in Fig. 2, and the conductance at these concentrations was estimated by extrapolating the current to zero time. No relaxations were observed with small applied voltages at the lower concentrations and these conductances were estimated from the steady state values of the currents observed on application of 10 mV. The current voltage curves are linear to 20 mV

the unstirred layers offering a greater diffusional resistance to the movement of the HA species than does the membrane.[2]

Relaxation Experiments

As illustrated in Fig. 1, we used the method of Stark *et al.* (1971) to obtain current relaxation curves following the application of a voltage pulse. An artist's tracing from a photograph of a current relaxation is illustrated in Fig. 4. The large capacitive spike (off record) decays with a time constant of about 1 μsec. Data were never analyzed from such relaxations for times less than 10 μsec. Similar relaxation curves obtained with slower time sweeps (not shown) demonstrated that the current was constant for times greater than 200 μsec. This confirmed that there was no significant diffusion polarization, a phenomenon which does occur at lower buffer concentrations.

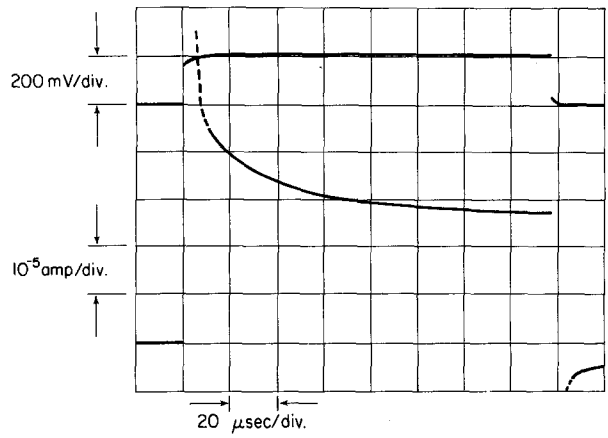

Fig. 4. An artist's tracing from a typical oscilloscope record obtained in a relaxation experiment. The bathing solutions contained 12.5 μM DTFB in 1 M NaCl buffered to pH 7.3. A 200-mV stimulus was applied and a current relaxation was observed, which was clearly distinct from the capacitive spike (time constant ~1 μsec)

2 We confirmed with an independent measurement that the aqueous unstirred layers rather than the membrane solution interfaces limit the movement of the HA species. We formed a PE bilayer membrane, then, while both aqueous phases were stirred at moderate speed, we added DTFB to one side of the membrane and measured the conductance. When the aqueous phase containing the DTFB was stirred rapidly and the other aqueous phase was not stirred, the conductance increased about a factor of two. When the aqueous phase containing the DTFB was not stirred and the other aqueous phase was stirred rapidly, the conductance fell by about a factor of two. These observations are consistent with the unstirred layers limiting the movement of HA through the membrane and are inconsistent with the interfaces limiting the movement. For additional discussion, references and a diagram, *see* McLaughlin and Eisenberg (1975), Fig. 2.

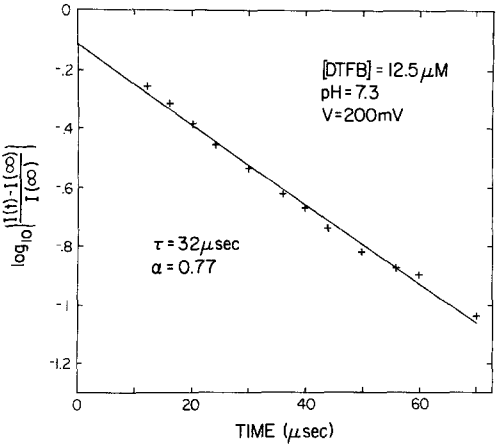

Fig. 5. A plot of the relaxation data obtained from Fig. 4. These data, which are represented by crosses, can be described by Eq. (9), which is represented by the straight line. *See text* for details

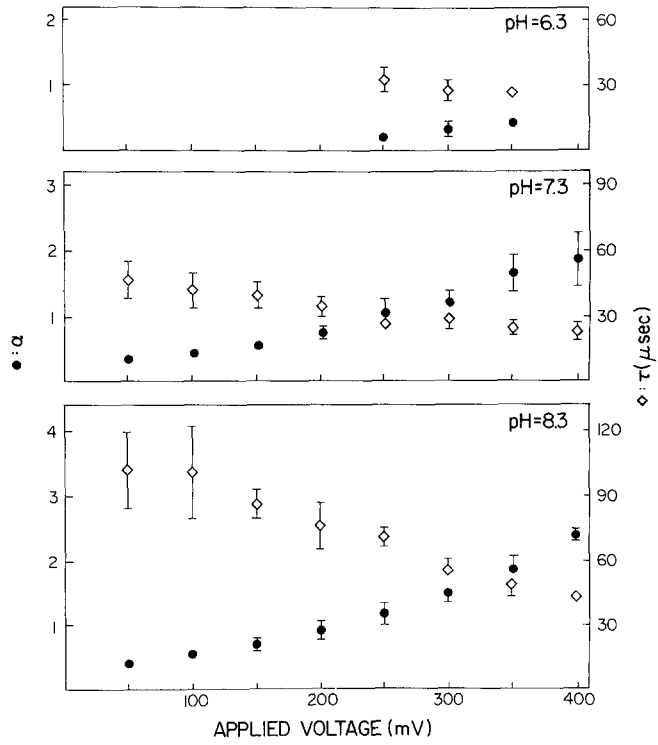

Fig. 6. Dependence of the relaxation amplitude, α, and the time constant, τ, on applied voltage. The black lipid membranes were formed from PE in a solution containing 12.5 μM DTFB buffered to the indicated pH. The error bars indicate the SD of at least three measurements

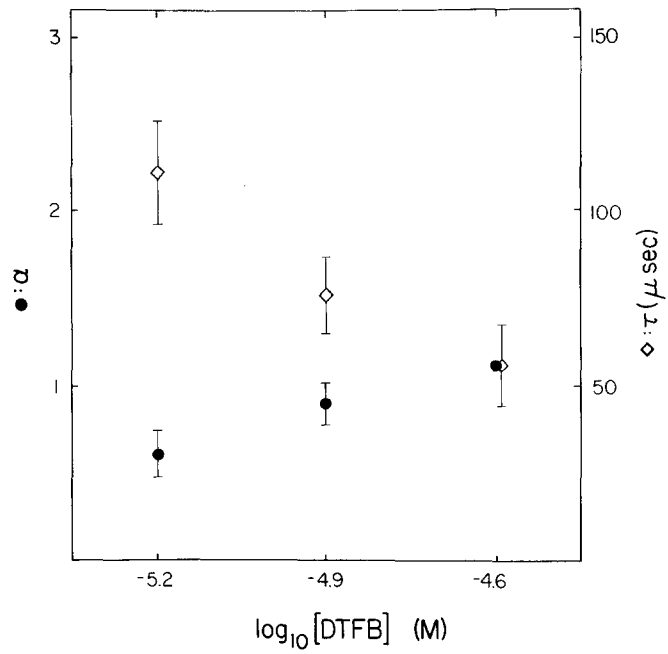

Fig. 7. Dependence of the relaxation amplitude, α, and time constant, τ, on the concentration of DTFB. The black lipid membranes were formed from PE in a solution buffered to pH = 8.3. A voltage pulse of 200 mV was applied to obtain the relaxation curves. The vertical bars indicate the SD of at least three measurements

The data in Fig. 4 were analyzed, as illustrated in Fig. 5, by plotting $\log_{10}\frac{I(t)-I(\infty)}{I(\infty)}$ against time where I(t) is the current at time t and $I(\infty)$ is the steady state current. The straight line in Fig. (5) is the least squares linear regression fit to the experimental data, as determined on a HP 9830 calculator. The fit is quite good, indicating that the data can be described by the equation:

$$I(t)=I(\infty)(1+\alpha e^{-t/\tau}) \tag{9}$$

where τ is the slope of the line in Fig. 5 (divided by $-\ln 10$) and α is the antilog of the ordinate intercept. We refer to τ as the *time constant* and to $\alpha=\frac{I(0)-I(\infty)}{I(\infty)}$ as the *relaxation amplitude.* We performed relaxation experiments, similar to the one illustrated in Fig. 4, at 50-mV intervals between 50 and 400 mV for three different values of the pH (6.3, 7.3 and 8.3) and three different values of the DTFB concentration (6.2, 12.5 and 25 μM). The data, when plotted in the manner illustrated in Fig. 5, could,

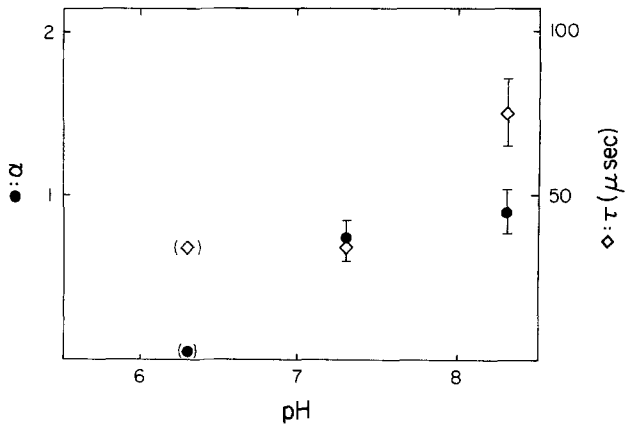

Fig. 8. The dependence of the relaxation amplitude, α, and the time constant, τ, on pH. The black lipid membranes were formed from PE in a solution containing 12.5 μM DTFB. A voltage pulse of 200 mV was applied to obtain the relaxation curves. The vertical bars indicate the SD of at least three measurements. The values in parentheses were calculated by extrapolation from the data in Fig. 6

in all cases, be fit well by straight lines. We discuss here the experimentally observed dependence of α and τ on voltage, [DTFB] and pH.

Fig. 6 illustrates the dependence of α and τ on voltage for three different values of the pH. Note that the relaxation amplitude, α, increases and that the time constant, τ, decreases as a function of the applied voltage.

Fig. 7 illustrates the dependence of α and τ on [DTFB] at pH 8.3, the pH where the concentration trends are most pronounced. It is apparent that α increases and τ decreases as [DTFB] increases.

Fig. 8 illustrates the dependence of α and τ on pH. Note that both the relaxation amplitude and time constant are larger at pH 8.3 than at pH 6.3, even though the initial conductances have identical values (Fig. 3).

Kinetic Theory

Description of the Model

All the equilibrium experimental data presented above are consistent with the postulate that a HA_2^- complex carries the current through the membrane interior. It is shown in *Appendix 1* that the diffusion of neither

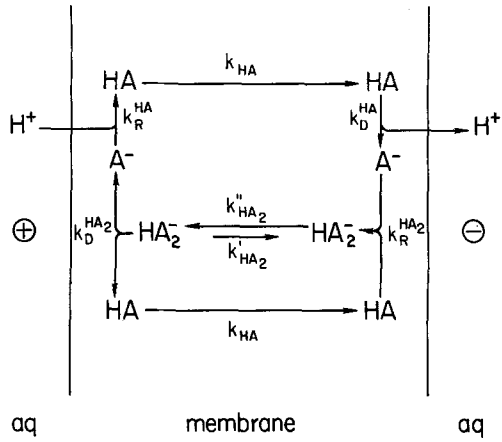

Fig. 9. Diagram illustrating the various reactions that are assumed to occur at the membrane solution interfaces with the indicated rate constants. The rate constants for the transmembrane processes are also illustrated. As indicated by the circled positive and negative signs, a voltage is assumed to be applied across the membrane. *See text* for details

the HA_2^- nor the A^- species through the unstirred layers could account for the experimentally observed steady state current. We conclude that buffered hydrogen ions diffuse through the unstirred layers and that the HA_2^- complex is formed at the membrane solution interface. The simplest model consistent with these conclusions is illustrated in Fig. 9, which is identical to the model proposed by Neumcke and Bamberg (1975) for the homologous uncoupler TTFB and to the model discussed by Smejtek, Hsu and Perman (1976) for pentachlorophenol.

We model the bilayer as a uniform slab of hydrocarbon with a thickness of 30 Å and denote the interior as the *membrane phase*. The A^-, HA and HA_2^- species are assumed to adsorb to the membrane-solution interface because of the amphipathic nature of DTFB. We assume that the interface is infinitely thin (the method of Gibbs; e.g., Aveyard and Haydon (1973) pp. 7–9), that the rates of the interfacial processes are independent of voltage and that the HA_2^- complex in the interior of the membrane responds to the entire applied voltage. The fluxes of the various species may be pictured in the following manner (Fig. 9). The buffered hydrogen ion diffuses through the left hand unstirred layer. It combines, at a rate described by the constant k_R^{HA}, with an A^- species adsorbed at the left hand interface. The resulting HA species diffuses from left to right with a rate constant k_{HA}. At the right hand interface HA decays into an aqueous H^+ and an interfacial A^- with a rate

constant k_D^{HA}. The interfacial HA and A^- combine with a rate constant $k_R^{HA_2}$ to form HA_2^-. Under the influence of the applied voltage, the HA_2^- species moves from right to left with a rate constant k''_{HA_2}, which is voltage dependent. At the left hand interface HA_2^- decays into an interfacial HA and A^- with a rate constant $k_D^{HA_2}$, and the cycle is repeated (the movement of HA_2^- against the applied voltage is described by the voltage dependent rate constant k'_{HA_2}). This cycle results in the movement of a H^+ ion from the left to the right aqueous phase.

We assume that the HA and HA_2^-, but not the A^-, species can partition into the membrane phase. We further assume that the adsorption onto the interface can be described by Henry's law for each of the three species. In particular, the adsorption coefficient of A^- is defined by $\gamma_A = [A^-]_{if}/[A^-]_{aq}$ where $[A^-]_{if}$ is the concentration of A^- at the membrane solution interface and $[A^-]_{aq}$ is the concentration of A^- in the aqueous phase. If the units of $[A^-]_{if}$ are moles/cm^2 and the units of $[A^-]_{aq}$ are moles/cm^3, γ_A is expressed in cm. The adsorption coefficient can be interpreted in the following manner. For a membrane of area S at equilibrium, each interface contains the same number of adsorbed A^- molecules as does the aqueous volume $S \times \gamma_A$. The adsorption coefficient of HA from the aqueous phase onto the interface, γ_{HA} is defined in a similar manner: $\gamma_{HA} = [HA]_{if}/[HA]_{aq}$. The adsorption coefficient of HA_2^- onto the interface is defined in a different manner. For the HA_2^- species, the ratio of the concentraton on the interface to the concentration in the center of the membrane phase is denoted by Γ_{HA_2}.

As discussed in more detail in *Appendix 2*, we used a Nernst-Planck treatment to describe the movement of HA_2^- through the interior of the membrane. We approximated the energy barrier that this species surmounts by a trapezoid. The movement of the HA species across the membrane interior at a rate k_{HA} was characterized by the permeability of the membrane to HA, $P_{HA} = \gamma_{HA} \times k_{HA}$. It was also assumed that the interfacially adsorbed HA and HA_2^- species were in equilibrium with their counterparts in the region of the membrane phase which was immediately adjacent to the interface.

The model is characterized by six nonlinear differential equations and has six independent variables which were chosen to be γ_A, γ_{HA}, Γ_{HA_2}, k_R^{HA}, $k_R^{HA_2}$ and P_{HA} *(Appendix 2)*. We sought numerical values for these parameters (consistent with certain physical constraints) that would give the best agreement between the theoretically predicted and experimentally observed decays of current with time at all values of the pH, [DTFB] and applied voltages.

Predictions of the Model

Fig. 10 shows three relaxation curves obtained by computer simulation. Note that the three curves can be fit quite well by a single exponential for times greater than 12 μsec. (Recall from Fig. 4 that experimental data were not obtained at times less than 10 μsec because of the large capacitive transient). At all applied voltages, pH values, and concentrations of DTFB, the theoretically predicted relaxation curves could be fit well by single exponentials. Nonlinear differential equations do not, in general, have exponential solutions. With rate constants and adsorption coefficients that give a "best" fit to our experimental data, however, one step of the cycle, the back diffusion of the neutral HA species, dominates the relaxation process. The best fit of our experimental data was obtained with the values of the rate constants and adsorption coefficients given in Table 1.

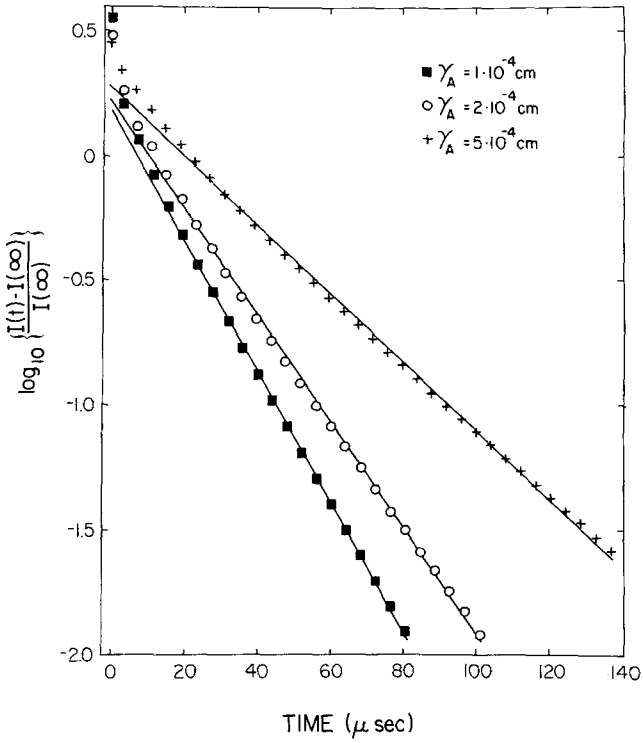

Fig. 10. Theoretical relaxation curves obtained by computer simulation. The applied voltage was assumed to be 200 mV, [DTFB] = 12.5 μM and pH = 7.3. All the rate constants and adsorption coefficients except γ_A were assumed to have the values listed in Table 1. γ_A was assumed to have the values indicated in the figure. The theoretical data were fit by straight lines by means of a least squares linear regression for times greater than 11 μsec. The values of α and τ deduced from Eq. 9 were: $\gamma_A = 1 \times 10^{-4}$, $\alpha = 1.5$, $\tau = 17$ μsec; $\gamma_A = 2 \times 10^{-4}$ cm, $\alpha = 1.7$, $\tau = 20$ μsec; $\gamma_A = 5 \times 10^{-4}$ cm, $\alpha = 1.9$, $\tau = 31$ μsec

Table 1. The rate constants and adsorption coefficients which give a best fit of the theoretically predicted relaxation curves to the experimental data

$\gamma_A = 2 \times 10^{-4}$ cm
$\gamma_{HA} = 2 \times 10^{-4}$ cm
$\Gamma_{HA_2} = 10^{-5}$ cm
$k_R^{HA} = 10^{16}$ cm^3 mole^{-1} sec^{-1}
$k_R^{HA_2} = 10^{17}$ cm^2 mole^{-1} sec^{-1}
$P_{HA} = 4$ cm sec^{-1}

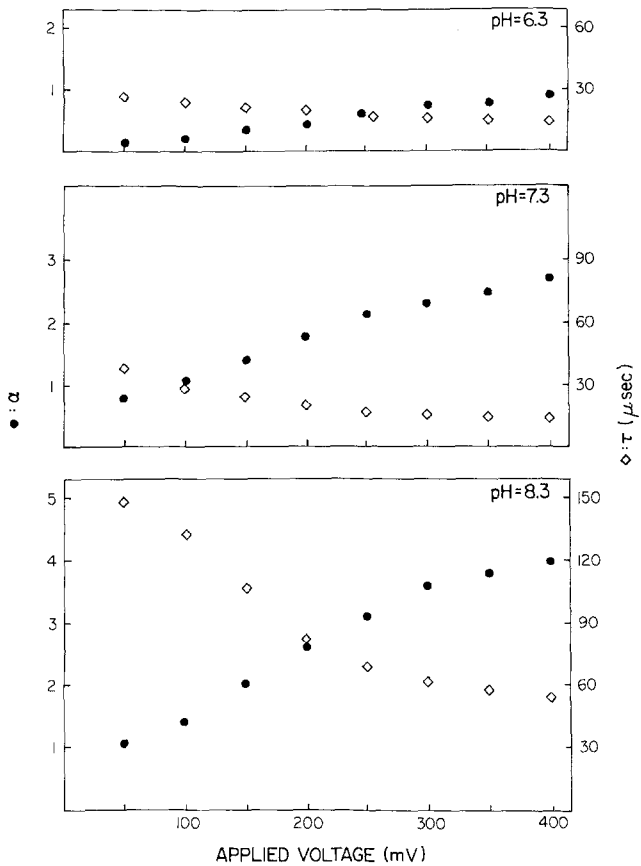

Fig. 11. The theoretically predicted dependence of α and τ on voltage for three different values of the pH. The concentration of DTFB was assumed to be 12.5 μM

In Fig. 11 the theoretically determined values of α and τ are graphed as a function of the applied voltage for three different values of the pH. The rate constants and adsorption coefficients were assumed to have the values listed in Table 1. At all values of the pH and [DTFB], α increases and τ decreases as the voltage increases, a prediction which agrees with

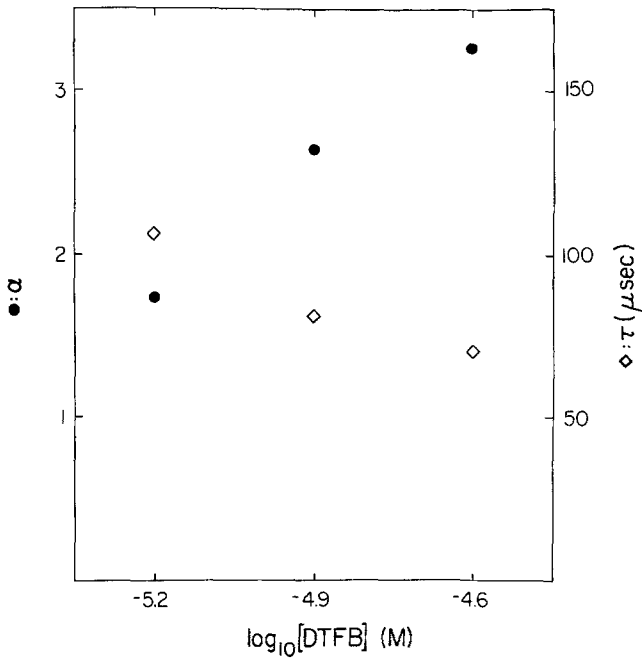

Fig. 12. The theoretically predicted dependence of α and τ on [DTFB]. The applied voltage was assumed to be 200 mV, and the pH was assumed to be 8.3. The rate constants and adsorption coefficients were assumed to have the values listed in Table 1

the experimental observations (Fig. 6). Quantitatively, the theoretical α is always larger than the experimental α, but the two agree within a factor of three.[3] The agreement between the theoretically predicted and experimentally observed values of τ is better, but again, far from perfect.

The theoretical dependence of α and τ on the concentration of DTFB is shown in Fig. 12. The predictions of the theory agree qualitatively with the experimental results (Fig. 7). Again, the theoretically predicted values of α are larger than the experimentally observed values. The agreement between the theoretically predicted and experimentally observed values of τ is somewhat better.

The predicted dependence of α and τ on pH is illustrated in Fig. 13. Qualitatively the theoretical predictions agree with the experimental observations (Fig. 8). The theoretically predicted and experimentally

3 The only way we have discovered to bring the theoretically predicted values of α into agreement with the experimentally observed values is to increase P_{HA} by about an order of magnitude. If, however, we assume that $P_{HA}=40$ cm/sec, it is necessary to also assume that $\gamma_A=\gamma_{HA}=5\times10^{-3}$ cm to preserve the agreement between the theoretically predicted and experimentally observed values of τ. As discussed in *Appendix 2* these values of P_{HA}, γ_A and γ_{HA} were considered physically unreasonable.

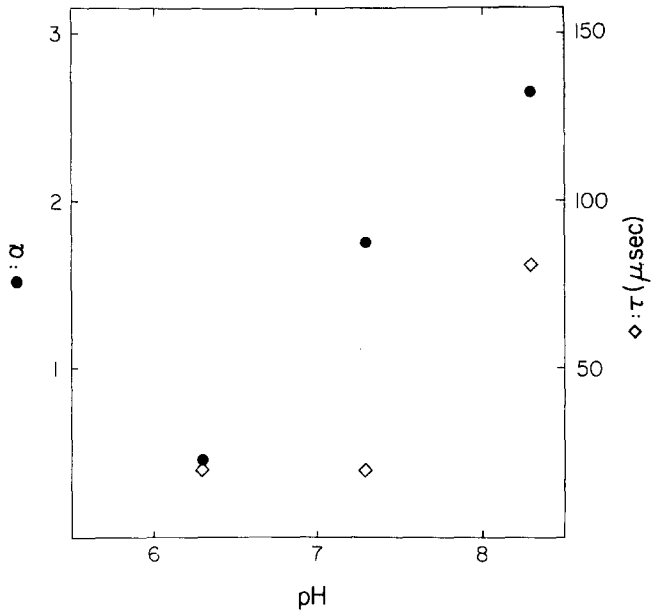

Fig. 13. The theoretically predicted dependence of α and τ on pH. The concentration of DTFB was assumed to be 12.5 μM and the applied voltage was assumed to be 200 mV. The adsorption coefficients and rate constants were assumed to have the values listed in Table 1

observed values of α increase with an increase in pH, whereas the values of τ are similar at pH 6.3 and 7.3 and larger at pH = 8.3.

The rate limiting process is the back diffusion of HA. We now discuss the rates of the processes illustrated in Fig. 9. By considering each of the second order steps in this model as a pseudo-first order process, we can compare the various rates. The rate at which H^+ crosses the interface is given by $[H^+]\, k_R^{HA}$. The rate at which the neutral HA species diffuses across the membrane interior is $k_{HA} = P_{HA}/\gamma_{HA}$. HA decays into an interfacially adsorbed A^- and an aqueous H^+ at a rate k_D^{HA}. The interfacially adsorbed A^- combines with an interfacially adsorbed HA to form HA_2^- at a rate $k_R^{HA_2}[A^-]_{if}$. The rate at which HA_2^- crosses the membrane interior from right to left is, as discussed in *Appendix 2*,

$$k''_{HA_2} = \{D^m_{HA_2}\, \phi\, e^{\phi/2}\}/\{2d\Gamma_{HA_2} \sinh(\beta\phi/2)\}.$$

The rate at which HA_2^- decays is $k_D^{HA_2}$. These rates are listed in descending order in Table 2. The only processes that will contribute to the observed relaxation of the current are those which occur at a rate

Table 2. Rates of the processes illustrated in Fig. 9, listed in descending order, for the assumed values of the rate constants listed in Table 1[a]

$k_D^{HA_2} = 4 \times 10^6\ sec^{-1}$
$k_D^{HA} = 1 \times 10^6\ sec^{-1}$
$k''_{HA_2} = 7 \times 10^5\ sec^{-1}$
$[H^+]\, k_R^{HA} = 5 \times 10^5\ sec^{-1}$
$[A^-]_{if}\, k_R^{HA_2} = 2 \times 10^5\ sec^{-1}$
$k_{HA} = 2 \times 10^4\ sec^{-1}$

[a] We assume that the pH is 7.3, that the concentration of DTFB is 12.5 μM, and that 200 mV is applied to the membrane

comparable to, or slower than, the rate at which HA_2^- is transported across the interior of the membrane. For our choice of parameters, we expect a fast relaxation due to interfacial processes and a slower relaxation due to the back diffusion (diffusion from the left to the right interface) of HA through the membrane phase.[4] This relaxation process is illustrated schematically in Fig. 14. The left hand side of Fig. 14 illustrates the equilibrium interfacial concentrations of the HA_2^-, HA and A^- species at pH 7.3. At the pH = pK, the aqueous concentrations of HA and A^- are, of course, identical. A best fit to our experimental data was obtained by assuming that the adsorption coefficients of HA and A^- were also identical (Table 1). Note that the interfacial concentration of HA_2^- is lower than that of either the HA or the A^- species. The right hand side of Fig. 14 illustrates the accumulation of the uncoupler at the left hand interface and the depletion of the uncoupler at the right hand interface when a steady state was obtained after the application of a voltage of 200 mV. These accumulations and depletions are, of course, due to the movement of the HA_2^- species across the membrane from right to left under the influence of an applied voltage. It is clear from Table 2 that the rate-limiting process is the diffusion of HA from the left hand interface to the right hand interface. The computer analysis predicts that at the right hand interface, the concentrations of A^-, HA and HA_2^- all decay to their steady state values with the same exponential time course seen for the current relaxation.[5] This occurs because the rates of

4 The predicted relaxations due to interfacial processes occur on a faster time scale (< 5 μsec) than we can resolve experimentally. If we were to assume somewhat faster interfacial kinetics, (e.g., increase either $k_R^{HA_2}$ or k_R^{HA}), then the predicted initial relaxation would become smaller and faster.

5 During the fast relaxation due to interfacial processes this statement is not correct. The time constants of these fast relaxations, however, are always less than 5 μsec (Table 2).

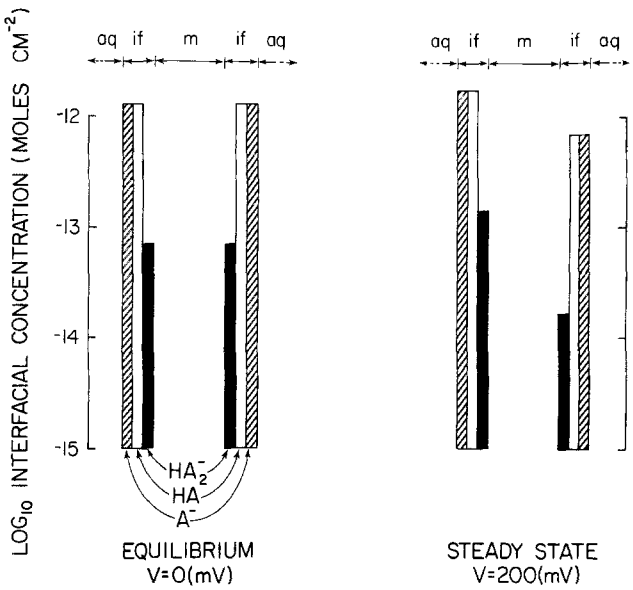

Fig. 14. *(Left):* The equilibrium interfacial (*if*) concentrations of the HA_2^-, HA and A^- species predicted by the theoretical model. The concentration of DTFB in the aqueous phases (*aq*) was assumed to be 12.5 μM and the pH was assumed to be 7.3. Note that both the HA and the A^- species adsorb strongly to the membrane solution interfaces. If, for example, the interfacially adsorbed HA were spread uniformly through the membrane phase (*m*) of thickness $d = 30$ Å, the partition coefficient into the membrane phase would be $2\gamma_{HA}/d \simeq 10^3$. The measured partition coefficient of the HA form of DTFB into decane is, however, only 1.2, which illustrates the importance of the interfaces in concentrating the uncoupler. *(Right):* The predicted steady state interfacial concentrations of the HA_2^-, HA and A^- species after the application of a 200-mV voltage pulse. The model predicts that the species maintain equilibrium among themselves at each interface. The concentrations of each species increase at the left and decrease at the right hand interface with the same time constant predicted for the decay of current. The back diffusion of the HA species from the right to the left hand interface is the rate limiting step. Our theoretical model assumes that there is a negligible flux of any of these species across the membrane-solution interfaces. This assumption can be shown to be consistent with a variety of experimental observations, one observation being the high interfacial adsorption of the HA and A^- species

the interfacial chemical reactions are fast compared to the rate at which the current decays to its steady state value.

Theoretical dependence of α and τ on various kinetic parameters. We now consider how changes in the kinetic parameters affect α, the relaxation amplitude. As the relaxation is due to the displaced HA back diffusing too slowly to maintain the interfacial concentrations constant, α will be affected only by those parameters that affect the flux of HA. As is illustrated in Fig. 10, variations in the adsorption coefficient of the A^-

species, γ_A, do not substantially affect α, the relaxation amplitude.[6] The results of the computer simulation verify that α is also relatively insensitive to variations in γ_{HA}, Γ_{HA_2}, k_R^{HA} and $k_R^{HA_2}$. The only parameter that affects α is P_{HA}.[7] Increases in P_{HA} result in decreases in α, whereas decreases in P_{HA} result in increases in α.[7] This prediction is consistent with the observation (data not shown) that the relaxation amplitude observed with the homologous uncoupler TTFB is smaller, at any given value of the pH measured relative to the pK, than the value of α measured with DTFB. The permeability of the neutral form of TTFB is higher than that of DTFB.

We now consider the dependence of the time constant, τ, on each of the kinetic parameters. To the extent that the interfacial processes can be considered sufficiently rapid with respect to the transmembrane processes, τ will be independent of both k_R^{HA} and $k_R^{HA_2}$. τ is, however, a function of γ_A and γ_{HA}. If either of these two adsorption coefficients increase, the corresponding interfacial equilibrium concentrations shown in the left hand side of Fig. 14 will increase. If we assume that the initial conductance of the membrane does not change and that the interfacial species maintain equilibrium among themselves, it follows that an increase in the interfacial adsorption of either HA or A^- will require more time for the concentrations to increase by a given fractional amount at the left hand interface and to decrease by a given fractional amount at the right hand interface. An increase in γ_A or γ_{HA} thus results in an increase in τ. The variation of τ with γ_A is easily seen in Fig. 10. For DTFB, τ is insensitive to variations in Γ_{HA_2} because the interfacial concentration of HA_2^- is small compared to the interfacial concentrations of either HA or A^-. An increase in the permeability of the membrane to HA will result in a decrease in τ.[8]

Intuitive explanations for the observed dependence of α and τ on pH. We compare the values of α and τ at pH 6.3 and 8.3 where the initial

6 If there were no fast relaxation due to interfacial processes, the theoretically predicted values of α would be completely independent of interfacial parameters. There is a fast relaxation and because variations in interfacial parameters do affect the size of the faster interfacial relaxation, there is a slight dependence of α on interfacial parameters.

7 We discovered, after we completed the computer analysis, that it is intuitively apparent that only P_{HA} can affect α if the back diffusion of the HA species is the rate limiting step. The predicted values of α are 3.2, 1.8, and 1.1 for $P_{HA}=2$, 4 and 8 cm/sec, respectively, when the other rate constants and adsorption coefficients have the values listed in Table 1.

8 For example, the predicted values of τ are 26, 20, and 14 μsec for $P_{HA}=2$, 4 and 8 cm/sec, respectively, when the other rate constants and adsorption coefficients have the values listed in Table 1.

conductances, $G_{V,0}$, are identical for a given [DTFB] and applied voltage. At pH = 6.3, 90% of the uncoupler in both the aqueous phases and the interfaces is in a neutral, HA, form; at pH = 8.3, only 10% of the uncoupler is in this form. As the interfacial concentrations of HA are high at pH = 6.3, a small percentage deviation of the interfacial concentrations from their equilibrium values can maintain a large back diffusional flux. Since the interfacial concentrations of HA are low at pH = 8.3, large percentage deviations of these interfacial concentrations are rquired to produce even a small back diffusional flux. When we apply a relatively large potential (e.g., 200 mV) the current is approximately proportional to the concentration of HA_2^- at the right hand interface (e.g., Eq. A.7). The charged permeant HA_2^- species, however, maintains equilibrium with the HA species at the interface. This means that if a large percentage decrease in the concentration of HA at the right hand interface (and, of course, a concomitant increase at the left hand interface) is required to produce a given back diffusional flux, a large percentage decrease in the concentration of HA_2^- will also result at the right hand interface. A large percentage decrease in concentration of HA_2^- at the right hand interface will produce a large percentage decrease in the current. The steady state current will, therefore, be lower at pH 8.3 than at pH 6.3 for a given concentration of uncoupler and applied voltage. Equivalently, the relaxation amplitude is larger at pH 8.3 than at 6.3. At a given [DTFB], pH and applied voltage, the time constant describing the change in concentrations is identical with the time constant describing the current relaxations. A given gradient of HA is established more rapidly at pH 6.3 than 8.3 because the HA_2^- that moves across the membrane decays mainly into HA at pH 6.3 but mainly into A^- at pH 8.3. The time constant for the current relaxation is, therefore, smaller at pH 6.3 than 8.3.

Independent Measurements

The model illustrated in Fig. 9 and defined by Eqs. (A.9–A.14) is definitely oversimplified and we were originally skeptical as to whether the parameters we deduced from the kinetic analysis had any physical significance. To test the model, we independently measured some of these parameters. All these independent measurements were made, for techni-

cal reasons, on the zwitterionic lipid phosphatidyl choline (PC) rather than phosphatidyl ethanolamine (PE)[9].

Estimate of P_{HA}. LeBlanc (1971) has demonstrated that one can determine the permeability of the bilayer to the neutral form of the acid by measuring the membrane potential, V, produced by a difference in pH. If we assume that the chemical reaction $H^+ + A^- \rightleftharpoons HA$ is at equilibrium within the unstirred layer and that the charged permeant species is the anion A^- when $pH \gg pK$, the membrane potential will be given by:

$$V = \frac{RT}{F} \ln \frac{(K_{HA} + [H^+]') + P_{HA}\delta[H^+]' S([H^+]', [H^+]'')}{(K_{HA} + [H^+]'') + P_{HA}\delta[H^+]'' S([H^+]', [H^+]'')} \tag{10}$$

where:

$$S([H^+]', [H^+]'') = \frac{K_{HA} + [H^+]'}{D_A K_{HA} + D_{HA}[H^+]'} + \frac{K_{HA} + [H^+]''}{D_A K_{HA} + D_{HA}[H^+]''}.$$

If we assume that the unstirred layer thickness is $\delta = 2 \times 10^{-2}$ cm (LeBlanc, 1971, Borisova *et al.*, 1974), and that the diffusion coefficients of both the neutral and charged species in the aqueous phase are $D_{HA} = D_A = 5 \times 10^{-6}$ cm^2/sec, the experimental data in Fig. 15 are fit well by Eq. (10) with $P_{HA} = 2$ cm/sec. (The fit is visually better for 2 than for either 1.5 or 2.5 cm/sec.) This value agrees as well as could be expected with the value of 4 cm/sec deduced from the kinetic measurements.

Estimate of γ_A: *Equilibrium dialysis.* Sonicated egg phosphatidyl choline vesicles were prepared as discussed above. They were placed in one side of a Teflon dialysis chamber, DTFB was added to either side, and the equilibrium concentration of DTFB in the side not containing the

9 We found that bacterial PE, in contrast to egg PC, did not form good sonnicated liposomes when prepared according to the method of Huang (1969). This necessitated the use of egg PC liposomes for the equilibrium dialysis measurements. For the measurements of P_{HA}, the membrane was exposed to solutions of $pH > 12$. In these alkaline solutions the primary amine group of PE, in contrast to the quaternary amine group of PC, would have been almost completely titrated (Szabo *et al.*, 1972). The planar membranes for these studies were, therefore, formed from PC. Finally, our samples of bacterial PE contained more negative contaminants than egg PC. The typical zeta potential of -30 mV seen with PE vesicles in a millimolar salt solution could be due, according to the Gouy equation, to 1% of the molecules in the vesicle bearing a negative charge. For these reasons, multilamellar vesicles for the electrophoresis experiments were formed from PC rather than PE. We used PE for the relaxation measurements because the dipole potential of PE is more positive (interior) than that of PC. This implies the conductance and the relaxations due to DTFB are larger in PE than PC membranes.

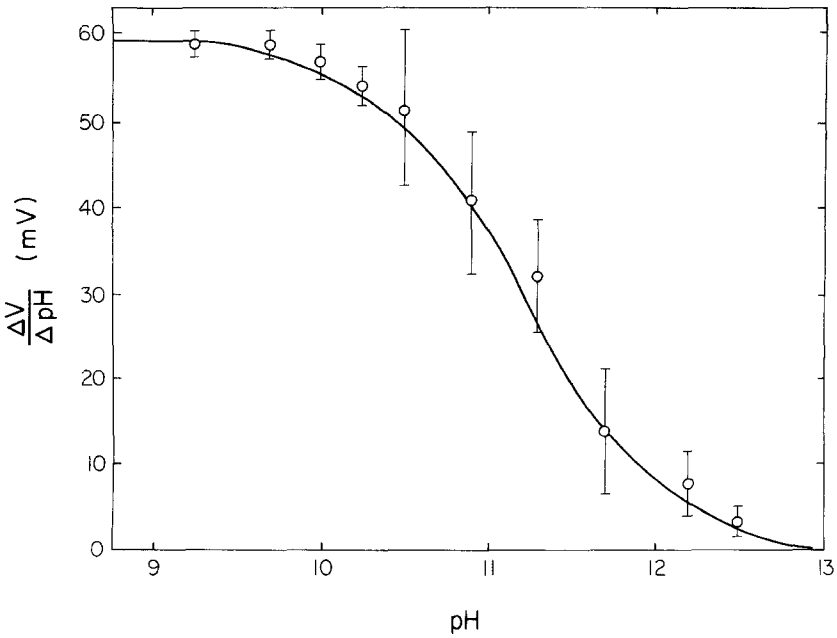

Fig. 15. Determination of P_{HA}. The membrane potential, V, was measured when the aqueous phases were of different pH and contained 25 μM DTFB. The aqueous solutions also contained 10^{-1} M NaCl, 10^{-1} M citrate, 10^{-1} M borate and 2×10^{-1} M phosphate. The error bars indicate the SD of at least three experiments

vesicles was determined spectrophotometrically. The experiment was done at several vesicle concentrations at pH 8.3, where 90% of DTFB is in the anionic form. We obtained a value of $(2.7 \pm 1.2) \times 10^{-4}$ cm for the adsorption coefficient of the anion by this direct measurement. This agrees well with the value of 2×10^{-4} cm deduced from a kinetic analysis of the relaxations.

Estimate of γ_A: *Electrophoresis.* Multilamellar egg phosphatidyl choline vesicles were prepared according to Bangham *et al.* (1974). They were suspended in a solution containing (in M) 10^{-3} NaCl, 10^{-4} tris and 10^{-4} NaH_2PO_4 buffered to pH 7.3, 8.0 or 9.1. We measured the electrophoretic mobility, then calculated the zeta potential (*see* Materials and Methods) from the Helmholtz-Smoluchowski equation. The estimated zeta potentials were 10.9 ± 3.2 mV (n = 30) at pH 7.3, 14.8 ± 7.2 (n = 10) at pH 8.0 and 21.3 ± 4.7 (n = 30) at pH 9.1. We then used the Stern equation (McLaughlin & Harary, 1976) to deduce the value of γ_A which was calculated to be 1.1, 1.1 and 1.5×10^{-4} cm at pH 7.3, 8.0 and 9.1, respectively. (The fact that similar results were obtained at pH 7.3 and

9.1 demonstrates that the anion rather than the HA_2^- species is producing the negative zeta potential.) The adsorption coefficient deduced by this technique agrees well with the value measured via equilibrium dialysis and both of these estimates agree well with the number obtained from kinetic measurements.

Estimate of γ_{HA}: This parameter was estimated by making equilibrium dialysis measurements at pH 4.3 on egg phosphatidyl choline vesicles. We deduced a value of $(2.8 \pm 1.9) \times 10^{-4}$ cm, which agrees well with the value of 2×10^{-4} cm calculated from kinetic measurements.

Discussion

The model we have presented is capable of describing qualitatively all the relaxation data that we have obtained. The experimental values of the time constants and relaxation amplitudes agreed, within a factor of two and three, respectively, with the values predicted by the model (Eqs. (A.9)–(A.14) and Fig. 9). The model is admittedly oversimplified, but there is agreement, within a factor of two, between the values of the adsorption coefficients (γ_A and γ_{HA}) and permeability (P_{HA}) calculated from the kinetic model and the values of these parameters determined from independent measurements. This strongly suggests that the essential features of the model are correct[10]. Even for a dansylated analog of valinomycin, which has a simpler carrier mechanism than DTFB, the agreement between the results predicted by electrical relaxation measurements and those determined by independent fluorescent measurements is only good to an order of magnitude (Pohl, Knoll, Gisin & Stark, 1976).

The biological relevance of this study, and other studies in progress in this laboratory on homologous substituted benzimidazoles (e.g., TTFB),

10 The model predicts that a fast relaxation should occur in the current (Fig. 10). This predicted relaxation is too fast for us to resolve with our voltage clamp technique, but could be tested by making charge pulse measurements (e.g., Feldberg & Kissel, 1975; Benz & Läuger, 1976). This prediction is consistent with the experimental observation that the extrapolated values of $G_{V,0}$ become less steeply dependent on voltage as [DTFB] increases at pH 7.3. We do not wish, however, to suggest that all features of our model are well understood. In particular, the rate constant k_R^{HA} is anomalously high. By applying the analysis of Koutecky and Brdicka (1947) to our problem, we calculated that the value of this rate constant apparently exceeds diffusion limitation. The assumption implicit in this calculation was that the rate at which hydrogen ions can cross the membrane-solution interface is less than or equal to the rate at which they can diffuse across a plane in a bulk aqueous solution. The assumption is questionable for a number of reasons (e.g., Zundel, 1976).

hinges on the current debate about the validity of the chemiosmotic hypothesis. The chemiosmotic hypothesis predicts that the mechanism by which weak acids uncouple mitochondria is identical to the mechanism by which they transport hydrogen ions across artificial bilayer membranes. To critically test this prediction, it will be necessary to study how the ability of a given uncoupler to affect mitochondria depends on its concentration and the pH of the bathing medium. These dependences, and the relative efficacy of different uncouplers on mitochondria, should all be predictable from a knowledge of the kinetic mechanisms by which these molecules transport hydrogen ions across black lipid membranes.

We now briefly discuss some of the factors that must be considered in such a study. Even if one is studying an uncoupler added at equal concentrations to both sides of an artificial membrane separating two identical solutions, one must consider (i) whether, if the uncoupler is an anion, the charged permeant species is A^- or HA_2^-, a consideration which can depend on pH and the concentration of the uncoupler, (ii) whether the uncoupler adsorbs to the membrane and changes the electrostatic surface potential, by means of an effect on the double layer, dipole or boundary potentials (e.g., McLaughlin, 1977), (iii) whether the uncoupler is a cation (e.g., dibucaine) or an anion. The ability of anionic and cationic uncouplers to transport hydrogen ions will be affected in opposite directions by factors which change the surface potential (e.g., surface charge density; salt concentration), (iv) whether kinetic parameters affect the conductance.

When the uncoupler is added to one side of a topologically closed vesicle, and the electrical potential and pH on the inside and outside of the vesicle are different, the situation is more complicated. The electrochemical potentials of the A^- (and HA) species on each side of the membrane will not, in general, be identical in the steady state. In addition to the factors listed in the previous paragraph, one must also take into account the thickness of the unstirred layers, the value of the pK in relation to the pH on both sides of the membrane, the buffer capacity of the two aqueous media and the kinetic behavior of the uncoupler. Even if the reactions which occur at the interface are essentially at equilibrium, which appears to be the case for DTFB, one must also know the permeability of the membrane and its associated aqueous unstirred layers to the neutral and charged forms of the uncoupler to calculate the steady state distribution of the uncoupler.

For most uncouplers (e.g., salicylate, DTFB, TTFB) the measured values of these parameters imply that the concentrations of the neutral

form on both sides of the vesicle will be approximately equal in the steady state. The exception to this general statement is picrate. This uncoupler has such a low pK (0.3) and the permeability of the anion is so high ($P_A = 10^{-5}$ cm/sec) in relation to the permeability of the neutral form ($P_{HA} = 0.2$ cm/sec), that it is the anion rather than the neutral species which is distributed such that its electrochemical potentials are identical on both sides of the membrane (McLaughlin, *et al., in preparation*). This could explain why picrate uncouples submitochondrial particles but not mitochondria (Hanstein & Hatefi, 1974*a*).

Finally, we note that the recent suggestion by Green and coworkers (Kessler *et al.*, 1977) that uncouplers function "both as proton and cation carrier" is not compatible with the results of experiments on black lipid membranes. The uncoupler DTFB, like all other uncouplers which have been examined to date (e.g., LeBlanc, 1971; Borisova *et al.*, 1974; Foster & McLaughlin, 1974) produces a Nernst potential in response to a gradient of hydrogen ions (Fig. 15). This implies that the permeability ratio of sodium to hydrogen ions, as defined by the Goldman-Hodgkin-Katz equation, is essentially zero.

We thank C. Murawski for excellent technical assistance with some of the experiments and Dr. S. Feldberg for a valuable discussion about the computer program.

This work was supported by NSF grant PCM76-04363.

Appendix 1

In this appendix we argue that the flux of neither the A^- nor the HA_2^- species through the unstirred layers is sufficient to account for the experimentally observed steady state current. Neumcke and Bamberg (1975) have shown that the maximum steady state conductance, $G_{0,\infty}$, that can be supported by diffusion of HA_2^- through the unstirred layers is, at pH = pK:

$$G_{0,\infty} = \frac{F^2 D[A^{TOT}]^2}{4RT\delta K_{HA_2}} \tag{A.1}$$

provided that:

$$E\delta \gg 1 \tag{A.2}$$

where:

$$E^2 = (l_D + l_R[A^{TOT}])/D. \tag{A.3}$$

In these equations D is the value of the diffusion coefficient of the various uncoupler species in the aqueous phases, δ is the thickness of the unstirred layers, l_D is the dissociation rate constant for the reaction described by Eq. (2) and l_R is the recombination rate constant for the same process. If $[A^{TOT}]=12.5\,\mu M$, $\delta=2\times10^{-2}$ cm, $D=5\times10^{-6}$ cm^2/sec, $K_{HA_2}\geqq10^{-4}$ M (Eq. (4) implies that $K_{HA_2}\gg[A^{TOT}]$ in the region where the conductance depends quadratically on the concentration of DTFB), the maximum value for the conductance is calculated to be $G_{0,\infty}<4\times10^{-7}$ mho/cm^2. The experimentally observed value of the conductance (Fig. 2) can be as high as 4×10^{-2} mho/cm^2 and obviously cannot be accounted for by the diffusion of HA_2^- through the unstirred layers. In this calculation the chemical reactions which occur in the aqueous phases, Eqs. (1) and (2) were taken into account. Eq. (A.2) holds provided that either $l_D\gg5\times10^{-2}$ sec^{-1} or $l_R\gg4\times10^6$ cm^3 mole^{-1} sec^{-1}. If one of these inequalities is not obeyed, the calculated maximum value of the flux would have a lower value.

The maximum steady state conductance that could be supported by diffusion of A^- through the unstirred layers is (Neumcke & Bamberg, 1975):

$$G_{0,\infty}=\frac{F^2\sqrt{Dk_D}[A^-]}{4\sqrt{2}RT} \tag{A.4}$$

provided that:

$$Q\delta\gg1 \tag{A.5}$$

where:

$$Q^2=(k_D+k_R[H^+])/D\,. \tag{A.6}$$

In these equations k_D is the dissociation rate constant and k_R the recombination rate constant of the reaction described by Eq. (1) and $[A^-]$ is the concentration of A^- in the bulk aqueous phase. We ignore, in this calculation, the formation of the HA_2^- complex within the unstirred layers. If $[A^{TOT}]=12.5\,\mu M$, $D=5\times10^{-6}$ cm^2/sec, $k_R=10^{14}$ cm^3 mole^{-1} sec^{-1} and pH = 7.3, $G_{0,\infty}=1.5\times10^{-3}$ mho/cm^2. The experimentally observed maximum conductance is more than an order of magnitude higher than this calculated value. (If the inequality of Eq. (A.5) is not valid, a smaller conductance is predicted.)

Since the diffusion of neither the A^- nor the HA_2^- species could maintain the high steady state currents we observe, we are led to the conclusion that buffered hydrogen ions diffuse through the unstirred

layers. We assume that it is also H^+ which crosses the membrane solution interface (e.g., Fig. 9). More complicated mechanisms that would allow other species to cross the interface are considered unlikely (Cohen, 1976; Smejtek *et al.*, 1976).

Appendix 2

We discuss, in this appendix, the details of our kinetic model. The fluxes of both the HA and HA_2^- species through the membrane phase are described in terms of the Nernst-Planck electrodiffusion theory. The energy profiles for the HA, A^- and HA_2^- species are illustrated in Fig. 16. Note that the self energies (standard chemical potentials) of all species are assumed to be independent of distance in the aqueous phases. The interfaces are assumed to be infinitely thin, hence there can be no variation of the self energy within the interface. As the current carried through the interior of the membrane by the A^- species is negligible for $pH \leqq 8.3$, we assume that this species must surmount an infinitely high barrier in the membrane phase. We approximate the self energy of the neutral HA species through the membrane phase by a square barrier. If the charged permeant HA_2^- species also encountered a square barrier,

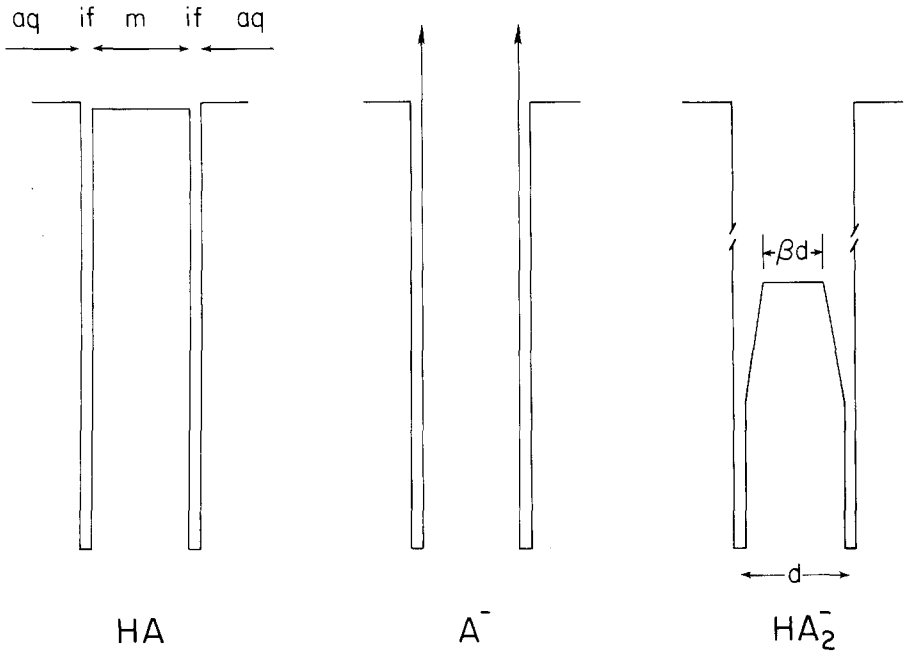

Fig. 16. Energy profiles for the HA, A^- and HA_2^- species. *See text* for details

the current-voltage curves would be linear. The experimental current-voltage curves, however, bend toward the current axis. This observation implies that the self energy of the HA_2^- species varies with distance through the membrane phase. If the variation is due mainly to image charge forces (Neumcke & Läuger, 1969; Haydon & Hladky, 1972; Andersen & Fuchs, 1975; Bradshaw & Robertson, 1975) the energy barrier can be approximated by a trapezoid, (e.g., Hall, Mead & Szabo, 1973; Ginsburg & Noble, 1976). If we ignore the Maxwell displacement current, the Nernst-Planck electrodiffusion theory and the constant field assumption predict that the dependence of conductance, $G_{V,t}$, on voltage, V, for a trapezoidal barrier is given by (Hladky, 1974):

$$G_{V,t}=\frac{F^2 D^m_{HA_2} e^{-\phi_0}}{2RTd}\,\frac{[HA_2^-]''_m e^{\phi/2}-[HA_2^-]'_m e^{-\phi/2}}{\sinh(\beta\phi/2)} \tag{A.7}$$

where $\phi=FV/RT$, $[HA_2^-]'_m$ is the concentration at the left hand edge of the membrane phase, $[HA_2^-]''_m$ is the concentration at the right hand edge of the membrane phase ϕ_0, is, in dimensionless units, the difference in the self energy of a HA_2^- ion in the center and at the edge of the membrane phase, β is the fraction of the membrane phase spanned by the minor base of the trapezoid, d is the thickness of the membrane phase, and $D^m_{HA_2}$ is the diffusion coefficient of the HA_2^- species in the membrane phase.

For simplicity, we assumed that both the HA and HA_2^- species at each of the interfaces maintained equilibrium with their counterparts in the membrane phase immediately adjacent to the interface. For example, at the left hand interface, we assumed that:

$$[HA_2^-]'_{if}=\Gamma_{HA_2} e^{-\phi_0}[HA_2^-]'_m \tag{A.8}$$

was true at all times.

The model is described by the following six differential equations:

$$\frac{d[HA_2^-]'_{if}}{dt}=-k'_{HA_2}[HA_2^-]'_{if}+k''_{HA_2}[HA_2^-]''_{if}+k_R^{HA_2}[A^-]'_{if}[HA]'_{if}-k_D^{HA_2}[HA_2^-]'_{if} \tag{A.9}$$

$$\frac{d[HA]'_{if}}{dt}=\frac{P_{HA}}{\gamma_{HA}}([HA]''_{if}-[HA]'_{if})+k_R^{HA}[H^+]'_{aq}[A^-]'_{if}-k_D^{HA}[HA]'_{if}-k_R^{HA_2}[A^-]'_{if}[HA]'_{if}+k_D^{HA_2}[HA_2^-]'_{if} \tag{A.10}$$

$$\frac{d[A^-]'_{if}}{dt} = -k_R^{HA}[H^+]'_{aq}[A^-]'_{if} + k_D^{HA}[HA]'_{if} - k_R^{HA_2}[A^-]'_{if}[HA]'_{if} + k_D^{HA_2}[HA_2^-]'_{if} \quad (A.11)$$

$$\frac{d[HA_2^-]''_{if}}{dt} = k'_{HA_2}[HA_2^-]'_{if} - k''_{HA_2}[HA_2^-]''_{if} + k_R^{HA_2}[HA]''_{if}[A^-]''_{if} - k_D^{HA_2}[HA_2^-]''_{if} \quad (A.12)$$

$$\frac{d[HA]''_{if}}{dt} = -\frac{P_{HA}}{\gamma_{HA}}([HA]''_{if} - [HA]'_{if}) + k_R^{HA}[H^+]''_{aq}[A^-]''_{if} - k_D^{HA}[HA]''_{if} - k_R^{HA_2}[A^-]''_{if}[HA]''_{if} + k_D^{HA_2}[HA_2^-]''_{if} \quad (A.13)$$

$$\frac{d[A^-]''_{if}}{dt} = -k_R^{HA}[H^+]''_{aq}[A^-]''_{if} + k_D^{HA}[HA]''_{if} - k_R^{HA_2}[A^-]''_{if}[HA]''_{if} + k_D^{HA_2}[HA_2^-]''_{if} \quad (A.14)$$

where

$$k'_{HA_2} = \{D^m_{HA_2}\,\phi\, e^{-\phi/2}\}/\{2d\Gamma_{HA_2}\sinh(\beta\phi/2)\}$$

and

$$k''_{HA_2} = \{D^m_{HA_2}\,\phi\, e^{\phi/2}\}/\{2d\Gamma_{HA_2}\sinh(\beta\phi/2)\}$$

The model contains the following eleven undetermined parameters: d, $D^m_{HA_2}$, β, k_D^{HA}, $k_D^{HA_2}$, γ_A, γ_{HA}, Γ_{HA_2}, P_{HA}, k_R^{HA} and $k_R^{HA_2}$. We assumed that the thickness of the membrane phase, d, was 30 Å, that the value of the diffusion coefficient of HA_2^- within the membrane, $D^m_{HA_2}$, was independent of position and that it was equal to 10^{-7} cm^2/sec.[11] The value of β was determined from the experimental current-voltage curves to be about 0.77.[12] The equilibrium value of $[HA_2^-]_{if}$ was determined by

11 The conclusions of this paper were not significantly altered by choosing different values for the diffusion coefficient of the HA_2^- species within the membrane (at least up to one order of magnitude) if $G_{V,0}$ was maintained a constant by varying Γ_{HA_2}.

12 From Eq. (A.7) it is apparent that: $G_{V,0}/G_{0,0} = \frac{\beta\sinh(\phi/2)}{\sinh(\beta\phi/2)}$. A best fit to the experimental $G_{V,0}/G_{0,0}$ data, for $\phi = FV/RT \leqq 6$ was obtained with $\beta = 0.77$. The data were not, however, described well by this equation over the entire voltage range. The experimental data obtained at higher voltages were better described with a higher value of β (e.g., $\beta = 0.85$). Our protocol was to fix $\beta = 0.77$, $d = 30$ Å, and $D^m_{HA_2} = 10^{-7}$ cm^2/sec. A combination Eq. (A.8) and (A.7) results in an expression for $G_{V,t}$ as a function of $[HA_2^-]'_{if}$, $[HA_2^-]''_{if}$ and Γ_{HA_2}. At $t=0$, $[HA_2^-]'_{if} = [HA_2^-]''_{if}$. A particular guess for Γ_{HA_2} and the experimental value of $G_{V,0}$ were then used to determine the value of $[HA_2^-]_{if}$ at $t=0$. The theoretically predicted values for the current as a function of time could then be determined from the numerical solution to Eqs. (A.9)–(A.14). This protocol results in the calculated values of $[HA_2^-]_{if}$ at $t=0$ being slightly (10%) dependent on voltage. This result is without serious consequence because neither α nor τ depend strongly on the value of $[HA_2^-]_{if}$ for a given value of the intitial current. We confirmed that different choices of β ($0.72 < \beta < 0.85$) gave similar (within 1%) values for α and τ for a given set of rate constants, adsorption coefficients and initial current.

inserting the experimental value of $G_{V,0}$ and a particular guess for the value of Γ_{HA_2} into Eqs. (A.7) and (A.8). The equilibrium values of $[A^-]_{if}$ and $[HA]_{if}$ were determined, at a given value of the pH and [DTFB], by making particular guesses for the values of γ_A and γ_{HA}. These concentrations determined the equilibrium constants for the interfacial reactions. Particular guesses for the values of k_R^{HA} and $k_R^{HA_2}$, therefore, determined k_D^{HA} and $k_D^{HA_2}$. In this manner, the number of independent parameters was reduced from 11 to 6, specifically: γ_A, γ_{HA}, Γ_{HA_2}, P_{HA}, k_R^{HA}, $k_R^{HA_2}$. Assignment of numerical values to these six parameters allowed us to generate theoretical current-time relaxation curves for different values of the voltage, pH and [DTFB].

The set of differential equations describing the model (Eqs. (A.9)–(A.14) may be represented as:

$$\frac{dY}{dt} = f(Y,t) \tag{A.15}$$

where Y denotes a column vector of the various concentrations. Eq. (A.15) can be written in an explicit form:

$$\Delta Y = f(Y,t)\,\Delta t \tag{A.16}$$

or in an implicit form:

$$\Delta Y = f(Y + b\Delta Y, t)\,\Delta t \tag{A.17}$$

where

$$0 < b \leqq 1.$$

A computer program utilizing an implicit routine was, as suggested to us by Dr. S. Feldberg, several times faster than an explicit Runge-Kutta routine. The implicit routine allowed us to use a coarser time mesh to solve the equations. We checked, with a desk calculator, that the numerical solutions we obtained with both methods did satisfy the differential equations. Cohen (1976) may be consulted for a more extended discussion of the implicit routine used to solve these equations.

We searched for the set of rate constants and adsorption coefficients that gave the best agreement between the theoretically predicted and experimentally observed relaxation curves. Physically reasonable bounds were placed on some of the parameters. In particular, we did not allow the value of P_{HA} to exceed 4 cm/sec. (Foster & McLaughlin (1974) have determined that the partition coefficient of DTFB into bulk decane is 1.25. We assumed that the partition coefficient of DTFB into the membrane phase would be $0.12 < k^{HA} < 12$. We assumed that the diffusion

coefficient of the HA species in the membrane was $D^m_{HA} \leqq 10^{-7}$ cm^2/sec. Thus, from $P_{HA} = D^m_{HA} k^{HA}/d$ we obtained the constraint that $P_{HA} \leqq 4$ cm/sec.) We also required that γ_A and γ_{HA} be low enough for Henry's law to be valid. (We observed a quadratic dependence of conductance on concentration (Fig. 2). This implies that the number of A^- and HA molecules adsorbed to the membrane varied linearly with the aqueous concentration of uncoupler. If the maximum interfacial concentrations of these species were less than one molecule per 60 Å^2, about the area of a phospholipid molecule, the number of adsorbed molecules must be less than 1/600 Å^2 for Henry's law to be approximately valid. For [DTFB] $= 25\,\mu$M we obtain the contraint $\gamma_A, \gamma_{HA} < 2 \times 10^{-3}$ cm.) Finally, the value of $k_R^{HA_2}$ was assumed not to exceed diffusion limitation. We comment on the large apparent value of k_R^{HA} in footnote 10.

References

Acheson, R.M., Taylor, G.A., Tomlinson, M.L. 1958. The synthesis of some benzimidazoles. *J. Chem. Soc.* **195**:3750

Anderson, O.S., Fuchs, M. 1975. Potential energy barriers to ion transport within lipid bilayers: Studies with tetraphenylborate. *Biophys. J.* **15**:795

Aveyard, R., Haydon, D.A. 1973. An introduction to the principles of surface chemistry. Cambridge University Press, Cambridge

Bamberg, E. 1973. Elektrochemische Untersuchungen an bimolekularen Lipidmembranen in Gegenwart von Entkopplern der oxidativen Phosphorylierung, Ph. D. Thesis. Universität Basel, Switzerland

Bangham, A.D., Flemans, R., Heard, D.H., Seaman, G.V.F. 1958. An apparatus for micro-electrophoresis of small particles. *Nature (London)* **182**:642

Bangham, A.D., Hill, M.W., Miller, N.G.A. 1974. Preparation and use of liposomes as models of biological membranes. *Methods Membr. Biol.* **1**:1

Benz, R., Läuger, P. 1976. Kinetic analysis of carrier-mediated ion transport by the charge-pulse technique. *J. Membrane Biol.* **27**:171

Blazyk, J.F., Steim, J.M. 1972. Phase transitions in mammalian membranes. *Biochim. Biophys. Acta* **266**:737

Borisova, M.P., Ermishkin, L.N., Liberman, E.A., Silberstein, A.Y., Trofimov, E.M. 1974. Mechanism of conductivity of bimolecular lipid membranes in the presence of tetrachlorotrifluoromethylbenzimidazole. *J. Membrane Biol.* **18**:243

Bradshaw, R.W., Robertson, C.R. 1975. Effect of ionic polarizability on electrodiffusion in lipid bilayer membranes. *J. Membrane Biol.* **25**:93

Büchel, K.H., Korte, F., Beechey, R.B. 1965. Uncoupling of the oxidative phosphorylation in mitochondria by NH-acidic benzimidazoles. *Angew. Chem. Int. Ed. Eng.* **4**:788

Ciani, S.M., Eisenman, G., Laprade, R., Szabo, G. 1973. Theoretical analysis of carrier mediated properties of bilayer membranes. *In:* Membranes. G. Eisenman, editor. Vol. 2, p. 61. Marcel Dekker, New York

Cohen, F.S. 1976. The mechanism of H^+ transfer across black lipid membranes mediated by an uncoupler of oxidative phosphorylation. A kinetic study with 5,6-dichloro-2-trifluoromethylbenzimidazole (DTFB). Ph. D. Thesis, S.U.N.Y. at Stony Brook

Cunarro, J., Weiner, M.W. 1975. Mechanism of action of agents which uncouple oxidative phosphorylation: Direct correlation between proton-carrying and respiratory-releasing properties using rat liver mitochondria. *Biochim. Biophys. Acta* **387**:234

Feldberg, S.W., Kissel, G. 1975. Charge pulse studies of transport phenomena in bilayer membranes. I. Steady-state measurements of actin- and valinomycin-mediated transport in glycerol monooleate bilayers. *J. Membrane Biol.* **20**:269

Finkelstein, A. 1970. Weak-acid uncouplers of oxidative phosphorylation. Mechanism of action on thin lipid membranes. *Biochim. Biophys. Acta* **205**:1

Foster, M., McLaughlin, S. 1974. Complexes between uncouplers of oxidative phosphorylation. *J. Membrane Biol.* **17**:155

Ginsburg, S., Noble, D. 1976. Use of current-voltage diagrams in locating peak energy barriers in cell membranes. *J. Membrane Biol.* **29**:211

Greville, G.D. 1969. A scrutiny of Mitchell's chemiosmotic hypothesis of respiratory chain and photosynthetic phosphorylation. *Curr. Top. Bioenerget.* **3**:1

Hall, J.E., Mead, C.A., Szabo, G. 1973. A barrier model for current flow in lipid bilayer membranes. *J. Membrane Biol.* **11**:75

Hanstein, W.G. 1976. Uncoupling of oxidative phosphorylation. *Biochim. Biophys. Acta* **456**:129

Hanstein, W.G., Hatefi, Y. 1974*a*. Trinitrophenol: A membrane-impermeable uncoupler of oxidative phosphorylation *Proc. Nat. Acad. Sci. USA* **71**:288

Hanstein, W.G., Hatefi, Y. 1974*b*. Characterization and localization of mitochondrial uncoupler binding sites with an uncoupler capable of photoaffinity labeling. *J. Biol. Chem.* **249**:1356

Harold, F.M. 1972. Conservation and transformation of energy by bacterial membranes. *Bacteriol. Rev.* **36**:172

Haydon, D.A., Hladky, S.B. 1972. Ion transport across thin lipid membranes: A critical discussion of mechanisms in selected systems. *Q. Rev. Biophys.* **5**:187

Hladky, S.B. 1974. The energy barriers to ion transport by nonactin across thin lipid membranes. *Biochim. Biophys. Acta* **352**:71

Hsia, J.C., Chen, W.L., Long, R.A., Wong, L.T., Kalow, W. 1972. Existence of phospholipid bilayer structure in the inner membrane of mitochondria. *Proc. Nat. Acad. Sci. USA* **69**:3412

Huang, C. 1969. Studies on phosphatidylcholine vesicles. Formation and physical characteristics. *Biochemistry* **8**:344

Kessler, R.J., Tyson, C., Zande, H. van de, Glasser, P., Green, D.E. 1977. Molecular mechanism of action of uncoupler (U) on mitochondrial coupler processes. *Biophys. J.* **17**:256*a*

Ketterer, B., Neumcke, B., Läuger, P. 1971. Transport mechanism of hydrophobic ions through lipid bilayer membranes. *J. Membrane Biol.* **5**:225

Koutecky, J., Brdicka, R. 1947. Fundamental equation for the electrolytic current when depending on the formation rate of the depolarizer jointly with diffusion and its polarographic verification. *Collect. Czech. Chem. Commun.* **12**:337

Kraayenhof, R., Arents, J.C. 1977. Fluorescent probes for the chloroplast energized state. Energy-linked change of membrane-surface charge. *In:* Electrical Phenomena at the Biological Membrane Level. E. Roux, editor. Elsevier, Amsterdam

Lea, E.J.A., Croghan, P.C. 1969. The effect of 2,4-dinitrophenol on the properties of thin phospholipid films. *J. Membrane Biol.* **1**:225

LeBlanc, O.H., Jr. 1971. The effect of uncouplers of oxidative phosphorylation on lipid bilayer membranes: Carbonylcyanide *m*-chlorophenylhydrazone. *J. Membrane Biol.* **4**:227

Liberman, E.A., Topaly, V.P., Tsofina, L.M., Jasaitis, A.A., Skulachev, V.P. 1969. Mechanism of coupling of oxidative phosphorylation and the membrane potential of mitochondria. *Nature (London)* **222**:1076

McLaughlin, S. 1972. The mechanism of action of DNP on phospholipid bilayer membranes. *J. Membrane Biol.* **9**:361

McLaughlin, S. 1977. Electrostatic potentials at membrane-solution interfaces. *In:* Current Topics in Membranes and Transport. F. Bonner and A. Kleinzeller, editors. Vol. 9, p. 71. Academic Press, New York

McLaughlin, S., Eisenberg, M. 1975. Antibiotics and membrane biology. *Annu. Rev. Biophys. Bioeng.* **4**:335

McLaughlin, S., Harary, H. 1976. The hydrophobic adsorption of charged molecules to bilayer membranes: A test of the applicability of the Stern equation. *Biochemistry* **15**:1941

Mitchell, P. 1961. Coupling of phosphorylation to electron and hydrogen transfer by a chemiosmotic type of mechanism. *Nature (London)* **191**:144

Mitchell, P. 1966. Chemiosmotic coupling in oxidative and photosynthetic phosphorylation. *Biol. Rev.* **41**:445

Mitchell, P. 1972. Chemiosmotic coupling in energy transduction: A logical development of biochemical knowledge. *Bioenergetics* **3**:5

Mitchell, P., Moyle, J. 1967*a*. Respiration-driven proton translocation in rat liver mitochondria. *Biochem. J.* **105**:1147

Mitchell, P., Moyle, J. 1967*b*. Acid-base titration across the membrane system of rat liver mitochondria. Catalysis by uncouplers. *Biochem. J.* **104**:588

Neumcke, B., Bamberg, E. 1975. The action of uncouplers on lipid bilayer membranes. *In:* Lipid Bilayers and Biological Membranes: Dynamic Properties. G. Eisenman, editor, p. 215. Marcel Dekker, New York

Neumcke, B., Läuger, P. 1969. Nonlinear electrical effects in lipid bilayer membranes. II. Integration of the generalized Nernst-Planck equation. *Biophys. J.* **9**:1160

Overbeek, J.Th.G., Wiersema, P.H. 1967. The interpretation of electrophoretic mobilities. *In:* Electrophoresis: Theory, Methods, and Application. M. Bier, editor. Vol. II, p. 1. Academic Press, New York

Pohl, G.W., Knoll, W., Gisin, B.F., Stark, G. 1976. Optical and electrical studies on dansyllysine-valinomyosin in thin lipid membranes. *Biophys. Struct. Mech.* **2**:119

Racker, E. 1976. A New Look at Mechanisms in Bioenergetics. Academic Press, New York

Racker, E., Stoeckenius, W. 1974. Reconstitution of purple membrane vesicles catalyzing light-driven proton uptake and adenosine triphosphate formation. *J. Biol. Chem.* **249**:662

Shaw. D.J. 1969. Electrophoresis. Academic Press, New York

Singleton, W.S., Gray, M.S., Brown, M.L., White, J.L. 1965. Chromotographically homogeneous lecithin from egg phospholipids. *J. Am. Oil. Chem. Soc.* **42**:53

Skulachev, V.P. 1971. Energy transformations in the respiratory chain. *Curr. Top. Bioenerget.* **4**:127

Smejtek, P., Hsu, K., Perman, W.H. 1976. Electrical conductivity in lipid bilayer membranes induced by pentachlorophenol. *Biophys. J.* **16**:319

Stark, G., Ketterer, B., Benz, R., Läuger, P. 1971. The rate constants of valinomycin-mediated ion transport through thin lipid membranes. *Biophys. J.* **11**:981

Szabo, G., Eisenman, G., McLaughlin, S.G.A., Krasne, S. 1972. Ionic probes of membrane structures. *Ann. N.Y. Acad. Sci.* **195**:273

Ting, H.P., Wilson, D.G., Chance, B. 1970. Effects of uncouplers of oxidative phosphorylation on the specific conductance of bimolecular lipid membranes. *Arch. Biochem. Biophys.* **141**:141

Wilson, D.F., Brooks, E. 1970. Inhibition of mitochondrial respiration by hydroxylamine and its relation to energy conservation. *Biochemistry* **9**:1090

Zundel, G. 1976. Easily polarizable hydrogen bonds—their interactions with the environment—IR continuum and anomalous large proton conductivity. *In:* The Hydrogen Bond, Recent Developments in Theory and Experiments. P. Schuster, G. Zundel, C. Sandorfy, editors, p. 687. North Holland, New York